Journal of Sound and Vibration (2001) **247**(3), 379–387
doi:10.1006/jsvi.2000.3381, available online at http://www.idealibrary.com on IDEAL®

SOUND TRANSMISSION IN MUFFLERS WITH MULTIPLE PERFORATED CO-AXIAL PIPES

E. DOKUMACI

Department of Mechanical Engineering, Dokuz Eylul University, Bornova, 35100 Izmir, Turkey

(*Received* 15 *May* 2000, *and in final form* 21 *August* 2000)

Although there exists ample literature on the analysis of mufflers with parallel multiple perforated pipes, there is a surprising void of papers on acoustical modelling of mufflers employing multiple co-axial pipes. In the present paper, the distributed parameter method is extended for the analysis of mufflers employing multiple co-axial pipes. The theory is presented in a generality encompassing any number of co-axial perforated pipes. Implementation of the theory is shown on a resonator with two co-axial perforated pipes. Experimental validation of the predictions is provided for the case of zero mean flow.

1. INTRODUCTION

Mufflers with multiple perforated pipes are often used in engine exhaust lines to attenuate tailpipe noise emission. In practical designs, the perforated pipes are arranged in parallel or co-axially. Although there exists ample literature on the analysis of mufflers with parallel multiple perforated pipes, there is a surprising void of papers on acoustical modelling of mufflers employing multiple co-axial pipes. The present paper aims to extend the distributed parameter method, which has received considerable attention recently in the context of mufflers with parallel multiple perforated pipes [1], to mufflers having multiple co-axial perforated pipes. The analysis is based on the methodology of reference [2] and presents an application and experimental verification.

2. SOUND WAVE TRANSFER ACROSS A CO-AXIAL *n*-PIPE ELEMENT

Shown in Figure 1 is a co-axial 3-pipe element. This consists of two co-axial uniform perforated pipes enclosed in a solid pipe or casing. Generalization of this is $n-1$ co-axial perforated pipes in a solid casing, which is referred to as the co-axial n-pipe element. Assuming isentropic fundamental mode acoustic wave propagation, a uniform mean flow, and $\exp(-\mathrm{i}\omega t)$ time dependence for the fluctuating quantities, where i denotes that unit imaginary number, ω is the radian frequency and t is the time, the momentum and continuity equations for any one of the pipes in a co-axial n-pipe element can be expressed as, respectively,

$$\frac{\partial p}{\partial x}+\left(M\ \frac{\partial}{\partial x}-\mathrm{i}k\right)V=0,\quad \left(M\ \frac{\partial}{\partial x}-\mathrm{i}k\right)p+\frac{\partial V}{\partial x}=mc. \tag{1, 2}$$

Here, x denotes the pipe axis, p is the acoustic pressure, V is given by $V=\rho_0 c_0 v$, where v is the acoustic particle velocity, ρ_0 is the ambient density and c_0 is the speed of sound under

0022-460X/01/430379 + 09 $35.00/0

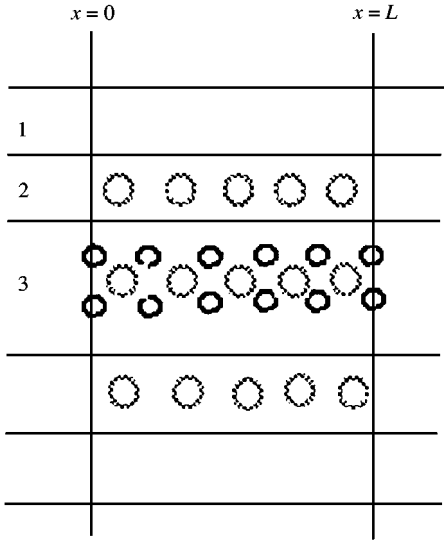

Figure 1. Co-axial 3-pipe element.

the ambient conditions, M is the mean flow Mach number, $M = v_0/c_0$, v_0 is the mean flow velocity, k is the wavenumber, $k = \omega/c_0$, and m is the mass injected into the pipe per unit volume per unit time. The latter is computed by conceiving the perforations as a continuous distribution over the pipe surface,

$$m = -a\Delta p/c_0, \quad a = \sigma P/S\zeta, \tag{3}$$

where Δp is the acoustic pressure difference across the perforate, σ is the perforate porosity, P is the perimeter of the pipe cross-sectional area, S, and ζ denotes the non-dimensional hole impedance, which is defined as $\zeta = \Delta p/\rho_0 c_0 u$, where u is the velocity of the fluid in the hole. It should be noted that a mean flow velocity gradient may be present in the designs employing a plugged pipe, however, the effect of this is generally small and can be taken into account sufficiently accurately by assuming an axially averaged uniform mean flow velocity [1, 2]. Thus, it is understood that, equations (1) and (2) are to be implemented by using an average mean flow velocity if there exists a mean flow velocity gradient along the pipe.

In applying equations (1) and (2) to a co-axial n-pipe element, pipes are numbered from 1 to n, pipe 1 always being the casing. The continuity and momentum equations for pipe j, where $j = 1, 2, \ldots, n$ throughout the analysis, can thus be expressed as

$$\left(M_j \frac{\partial}{\partial x} - \mathrm{i}k + a_j + b_{j+1}\right) p_j + \frac{\partial V_j}{\partial x} = a_j p_{j-1} + b_{j+1} p_{j+1}, \tag{4}$$

$$\frac{\partial p_j}{\partial x} + \left(M_j \frac{\partial}{\partial x} - \mathrm{i}k\right) V_j = 0, \tag{5}$$

where

$$a_j = \frac{\sigma_j P_j}{S_j \zeta_j}, \quad b_{j+1} = \frac{S_{j+1} a_{j+1}}{S_j}, \quad a_1 = b_{n+1} = 0. \tag{6}$$

Here, S_n is the cross-sectional area of pipe n, the most central pipe, S_j is the cross-sectional area of the annular space between pipe j and pipe $j + 1$, and P_j, σ_j and ζ_j are, respectively, the perimeter, the porosity and the hole impedance of pipe j. Note that $a_1 = b_{n+1} = 0$ and

$S_{n+1} = 0$ by definition. Equations (5) and (6) can be expressed concisely in matrix notation as

$$(\mathbf{A} + \mathbf{M}\,\partial/\partial x)\,\mathbf{Q} = 0, \tag{7}$$

where

$$\mathrm{A} = \begin{bmatrix} \mathbf{A}_{11} & \mathbf{A}_{12} & \mathbf{0} & \cdots & \mathbf{0} \\ \mathbf{A}_{21} & \mathbf{A}_{22} & \mathbf{A}_{23} & \cdots & \mathbf{0} \\ \mathbf{0} & \mathbf{A}_{32} & \mathbf{A}_{33} & \cdots & \mathbf{0} \\ \cdots & \cdots & \cdots & \cdots & \cdots \\ \mathbf{0} & \mathbf{0} & \mathbf{0} & \cdots & \mathbf{A}_{nn} \end{bmatrix}, \quad \mathbf{M} = \begin{bmatrix} \mathbf{M}_{11} & \mathbf{0} & \cdots & \mathbf{0} \\ \mathbf{0} & \mathbf{M}_{22} & \cdots & \mathbf{0} \\ \cdots & \cdots & \cdots & \cdots \\ \mathbf{0} & \mathbf{0} & \cdots & \mathbf{M}_{nn} \end{bmatrix}, \quad \mathbf{Q} = \begin{bmatrix} \mathbf{Q}_1 \\ \mathbf{Q}_2 \\ \mathbf{Q}_3 \\ \cdots \\ \mathbf{Q}_n \end{bmatrix}. \tag{8}$$

Here, $\mathbf{0}$ denotes a 2×2 matrix whose elements are all zero and

$$\mathbf{A}_{jj} = \begin{bmatrix} 0 & -\mathrm{i}k \\ -\mathrm{i}k + a_j + b_{j+1} & 0 \end{bmatrix}, \quad \mathbf{M}_{jj} = \begin{bmatrix} 1 & M_j \\ M_j & 1 \end{bmatrix}, \quad \mathbf{Q}_j = \begin{bmatrix} p_j \\ V_j \end{bmatrix}, \tag{9}$$

$$\mathbf{A}_{j+1,j} = \begin{bmatrix} 0 & 0 \\ -a_j & 0 \end{bmatrix}, \quad \mathbf{A}_{j,j+1} = \begin{bmatrix} 0 & 0 \\ -b_{j+1} & 0 \end{bmatrix}. \tag{10}$$

Equation (7) constitutes a set of $2n$ first order ordinary differential equations in variables p_j and V_j, $j = 1, 2, \ldots, n$. It is convenient to obtain the solution of these equations in terms of the pressure wave components p_j^+ and p_j^-, which correspond to waves travelling in forward, $+x$, and backward directions, respectively, and are defined for pipe j by the following transformation:

$$\begin{bmatrix} p_j(x) \\ V_j(x) \end{bmatrix} = \begin{bmatrix} 1 & 1 \\ 1 & -1 \end{bmatrix} \begin{bmatrix} p_j^+(x) \\ p_j^-(x) \end{bmatrix}, \tag{11}$$

or, briefly,

$$\mathbf{Q}_j = \mathbf{E}_j \mathbf{P}_j, \quad \mathbf{P}_j = \begin{bmatrix} p_j^+ \\ p_j^- \end{bmatrix}. \tag{12}$$

Clearly, here $\mathbf{E}_j$ denotes the square matrix in equation (11) and is the same for all pipes, however, the subscript is retained for notational convenience. With this transformation applied, equation (7) becomes

$$\frac{\partial \mathbf{P}}{\partial x} = \mathbf{H}\mathbf{P}, \quad \mathbf{H} = -\mathbf{E}^{-1}\mathbf{M}^{-1}\mathbf{A}\mathbf{E}, \quad \mathbf{P} = \begin{bmatrix} \mathbf{P}_1 \\ \mathbf{P}_2 \\ \cdots \\ \mathbf{P}_n \end{bmatrix}, \quad \mathbf{E} = \begin{bmatrix} \mathbf{E}_1 & \mathbf{0} & \cdots & \mathbf{0} \\ \mathbf{0} & \mathbf{E}_2 & \cdots & \mathbf{0} \\ \cdots & \cdots & \cdots & \cdots \\ \mathbf{0} & \mathbf{0} & \cdots & \mathbf{E}_n \end{bmatrix}. \tag{13}$$

Here, the system matrix $\mathbf{H}$ is

$$\mathbf{H} = \begin{bmatrix} \mathbf{H}_{11} & \mathbf{H}_{12} & \mathbf{0} & \cdots & \mathbf{0} \\ \mathbf{H}_{21} & \mathbf{H}_{22} & \mathbf{H}_{23} & \cdots & \mathbf{0} \\ \mathbf{0} & \mathbf{H}_{32} & \mathbf{H}_{33} & \cdots & \mathbf{0} \\ \cdots & \cdots & \cdots & \cdots & \cdots \\ \mathbf{0} & \mathbf{0} & \mathbf{0} & \cdots & \mathbf{H}_{nn} \end{bmatrix}, \tag{14}$$

where

$$2\mathbf{H}_{jj} = \begin{bmatrix} \dfrac{-\mathrm{i}2k + b_{j+1} + a_j}{1 + M_j} & \dfrac{b_{j+1} + a_j}{1 + M_j} \\ -\dfrac{b_{j+1} + a_j}{1 - M_j} & \dfrac{-\mathrm{i}2k + b_{j+1} + a_j}{1 - M_j} \end{bmatrix}, \tag{15}$$

$$2\mathbf{H}_{j+1,j} = \begin{bmatrix} \dfrac{-b_{j+1}}{1 + M_{j+1}} & \dfrac{-b_{j+1}}{1 + M_{j+1}} \\ \dfrac{b_{j+1}}{1 - M_{ij+1}} & \dfrac{b_{j+1}}{1 - M_{j+1}} \end{bmatrix}, \quad 2\mathbf{H}_{j,j+1} = \begin{bmatrix} \dfrac{-a_j}{1 + M_j} & \dfrac{-a_j}{1 + M_j} \\ \dfrac{a_j}{1 - M_j} & \dfrac{a_j}{1 - M_j} \end{bmatrix}. \tag{16, 17}$$

The general solution of this equation can be expressed as [3]

$$\mathbf{P}(x) = \exp(\mathbf{H}x)\mathbf{P}(0) = \Phi^{-1} \exp(\Lambda x)\Phi\mathbf{P}(0), \tag{18}$$

where Λ is a diagonal matrix of the $2n$ eigenvalues of matrix $\mathbf{H}$, and Φ is the corresponding modal matrix, the columns of which are the right eigenvectors of $\mathbf{H}$. A complex Jacobi algorithm is used to compute the eigenvalue and modal matrices. Thus, the sound wave transfer across a co-axial n-pipe element of length L can be expressed as

$$\mathbf{P}(L) = \mathbf{T}\mathbf{P}(0), \tag{19}$$

where the transfer matrix, $\mathbf{T}$, is computed from

$$\mathbf{T} = \Phi^{-1} \exp(\Lambda L)\Phi. \tag{20}$$

3. APPLICATION TO A RESONATOR

A resonator employing a co-axial 3-pipe element is shown in Figure 2. For acoustic modelling of this resonator, a relationship is required between $\mathbf{P}_3(0)$ and $\mathbf{P}_3(L)$, where L is the length of the perforated section. The first step in the formulation of this relationship is to derive a six-port for the perforated section by using equation (19). It is convenient to express the corresponding transfer matrix in partitioned form as

$$\begin{bmatrix} \mathbf{P}_1(L) \\ \mathbf{P}_2(L) \\ \mathbf{P}_3(L) \end{bmatrix} = \begin{bmatrix} \mathbf{T}_{11} & \mathbf{T}_{12} & \mathbf{T}_{13} \\ \mathbf{T}_{21} & \mathbf{T}_{22} & \mathbf{T}_{23} \\ \mathbf{T}_{31} & \mathbf{T}_{32} & \mathbf{T}_{33} \end{bmatrix} \begin{bmatrix} \mathbf{P}_1(0) \\ \mathbf{P}_2(0) \\ \mathbf{P}_3(0) \end{bmatrix}, \tag{21}$$

or, in expanded form,

$$\mathbf{P}_1(L) = \mathbf{T}_{11}\mathbf{P}_1(0) + \mathbf{T}_{12}\mathbf{P}_2(0) + \mathbf{T}_{13}\mathbf{P}_3(0), \tag{22}$$

$$\mathbf{P}_2(L) = \mathbf{T}_{21}\mathbf{P}_1(0) + \mathbf{T}_{22}\mathbf{P}_2(0) + \mathbf{T}_{23}\mathbf{P}_3(0), \tag{23}$$

$$\mathbf{P}_3(L) = \mathbf{T}_{31}\mathbf{P}_1(0) + \mathbf{T}_{32}\mathbf{P}_2(0) + \mathbf{T}_{33}\mathbf{P}_3(0). \tag{24}$$

The wave transfer relationship is then obtained by the application of the boundary conditions. Here the boundary conditions are expressed in terms of the reflection coefficient, R, which is defined as the quotient $R = p^-/p^+$. In this case, the reflection coefficients of the end-caps are given as boundary conditions and, therefore, $R_1(0)$, $R_2(0)$, $R_1(L)$ and $R_2(L)$ may be assumed to be known. Multiplying equations (22) and (23) from left by

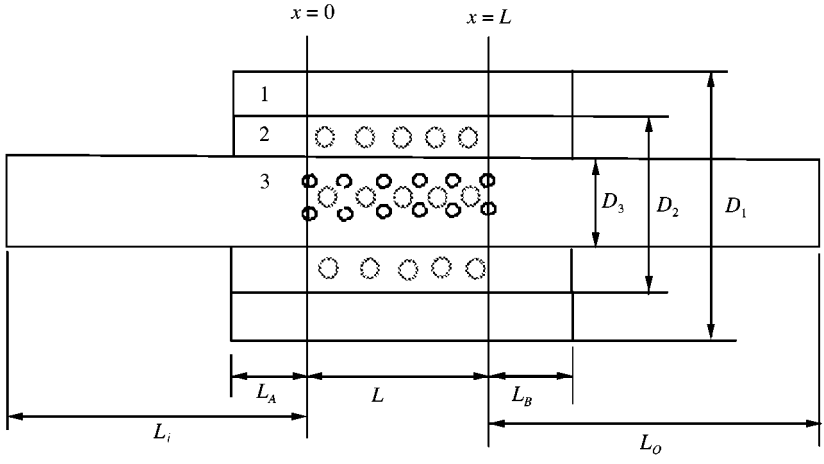

Figure 2. Resonator with two co-axial perforated pipes.

$\mathbf{Y}_1(L) = [R_1(L) \quad -1]$ and $\mathbf{Y}_2(L) = [R_2(L) \quad -1]$, respectively, yields

$$\mathbf{Y}_1(L)\mathbf{T}_{13}\mathbf{P}_3(0) + c_{11}p_1^+(0) + c_{12}p_2^+(0) = 0, \tag{25}$$

$$\mathbf{Y}_2(L)\mathbf{T}_{23}\mathbf{P}_3(0) + c_{21}p_1^+(0) + c_{22}p_2^+(0) = 0. \tag{26}$$

Here

$$c_{11} = \mathbf{Y}_1(L)\mathbf{T}_{11}\mathbf{R}_1(0), \quad c_{12} = \mathbf{Y}_1(L)\mathbf{T}_{12}\mathbf{R}_2(0), \tag{27}$$

$$c_{21} = \mathbf{Y}_2(L)\mathbf{T}_{21}\mathbf{R}_1(0), \quad c_{22} = \mathbf{Y}_2(L)\mathbf{T}_{22}\mathbf{R}_2(0), \tag{28}$$

where $\mathbf{R}_1(0) = \{1 \;\; \mathbf{R}_1(0)\}$ and $\mathbf{R}_2(0) = \{1 \;\; \mathbf{R}_2(0)\}$. Equations (25) and (26) can be solved to express $p_2^+(0)$ and $p_1^+(0)$ in terms of $\mathbf{P}_3(0)$:

$$p_1^+(0) = \mathbf{C}_1\mathbf{P}_3(0), \quad p_2^+(0) = \mathbf{C}_2\mathbf{P}_3(0), \tag{29}$$

Here,

$$(c_{22}c_{11} - c_{21}c_{12})\mathbf{C}_2 = -c_{22}\,\mathbf{Y}_1(L)\mathbf{T}_{13} + c_{12}\mathbf{Y}_2(L)\mathbf{T}_{23}, \tag{30}$$

$$(c_{22}c_{11} - c_{21}c_{12})\mathbf{C}_3 = c_{21}\,\mathbf{Y}_1(L)\mathbf{T}_{13} - c_{11}\mathbf{Y}_2(L)\mathbf{T}_{23}. \tag{31}$$

Hence, upon substituting equations (29) into equation (22),

$$\mathbf{P}_3(L) = [\mathbf{T}_{33} + \mathbf{T}_{32}\mathbf{R}_2(0)\mathbf{C}_2 + \mathbf{T}_{31}\mathbf{R}_3(0)\mathbf{C}_3]\mathbf{P}_3(0). \tag{32}$$

Clearly, the 2×2 matrix in square brackets is the required transfer matrix of the resonator.

Figure 3 presents the Noise Reduction characteristics of the resonator in Figure 2 (subsequently called 'co-axial resonator') with $L_1 = L_0 = 0{\cdot}555$ m long uniform inlet and outlet pipes, the latter having an un-flanged open termination. The Noise Reduction is defined as the level difference of the maximum sound pressure levels in the inlet and outlet pipes. Therefore, calculation of this also requires acoustic models of the inlet and outlet pipes and the open-end radiation condition. Isentropic fundamental mode propagation in a uniform pipe with uniform mean flow is given by equations (1) and (2) with $m = 0$. The formulation of the solution of these equations as a two-port relationship between the pressure wave components at the ends of the pipe is well known (this relationship is contained in the present formulation; it can be extracted by putting $j = 1$ and $a_2 = 0$ in

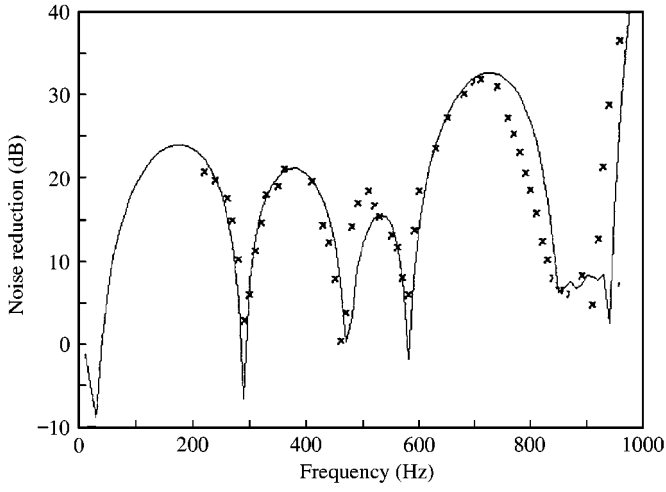

Figure 3. Noise reduction of the co-axial perforated pipe resonator: $M_1 = M_2 = M_3 = 0$ (——), Theory; × experiment. Resonator dimensions are: $L = 0{\cdot}3$ m, $L_A = L_B = 0{\cdot}037$ m, $D_3 = 0{\cdot}046$ m, $D_2 = 0{\cdot}153$ m, $D_1 = 0{\cdot}192$ m.

equation (14)). For the calculation of the noise reduction, the acoustic two-ports of the inlet and outlet pipes are first connected in cascade with equation (32) and the open-end radiation condition is applied to the outlet pipe. Then the standing waves in the inlet outlet pipes, and hence the noise reduction, are determined. The models used for the open-end radiation condition and perforate impedance are as described in reference [1]. The salient parameters of the resonator are as follows: $L = 0{\cdot}3$ m, $L_A = L_B = 0{\cdot}037$ m, $D_3 = 0{\cdot}046$ m, $D_2 = 0{\cdot}153$ m, $D_1 = 0{\cdot}192$ m, $d_3 = 0{\cdot}002$ m, $d_2 = 0{\cdot}003$ m, $t_3 = 0{\cdot}002$ m, $t_2 = 0{\cdot}0035$ m, $\sigma_3 = \sigma_2 = 0{\cdot}031$ and $M_1 = M_2 = M_3 = 0$, where d, t and D denote, respectively, the hole diameter, the wall-thickness and the internal diameter of a pipe. Also shown in Figure 3 is the measured noise reduction. Using a loudspeaker at the inlet of the inlet pipe excited the resonator and the measurements were carried out at room temperature by using the travelling microphone method. Measurements below 200 Hz could not be done accurately due to the limitations of the experimental set-up. The agreement between the predicted and measured noise reduction is fairly good.

In general, if the frequency is low enough, the noise reduction of a resonator with co-axial perforated pipes is similar to that of the same resonator without the co-axial pipe. Shown in Figure 4 are the noise reduction characteristics of the resonator of Figure 2 without the co-axial pipe (subsequently called "simple resonator") and without both perforated pipes (subsequently called "expansion chamber"), the salient parameters being the same as the co-axial resonator when applicable. It is seen that noise reduction of the simple resonator is the same as the expansion chamber up to about 200 Hz, and it is not discernible from that of the co-axial resonator up to about 650 Hz: that is, the inner and the outer perforated pipes are transparent acoustically below 200 and 650 Hz respectively (the cut-off frequency for the expansion chamber configuration is about 1000 Hz). Thus, insofar as sound reduction at relatively low frequencies is concerned, there is not much to be gained from the use of a perforated co-axial pipe of high porosity; however, such a perforated pipe may be employed as a shield for absorptive packing application in the outer annulus. The coupling between the adjacent annuli can become more marked with a co-axial pipe of low porosity, but this does not necessarily mean an overall improvement in sound reduction in a frequency range unless the annuli volumes are suitably chosen. Figure 5 shows the

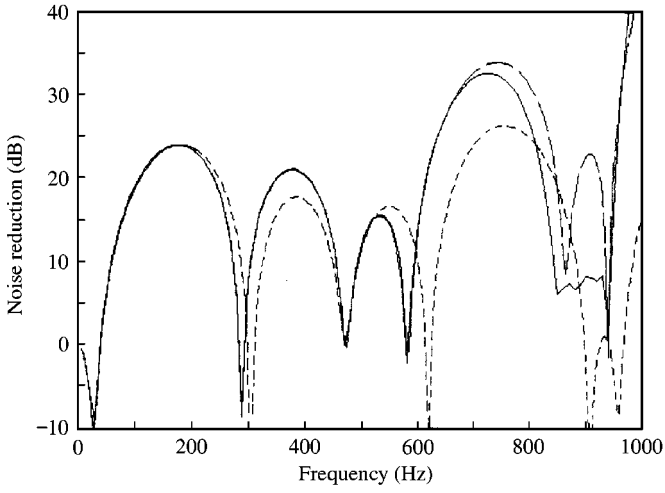

Figure 4. Noise reduction of the resonators derived from the co-axial resonator. (– – –), simple expansion chamber without any perforated pipes; (— — —), resonator without the co-axial perforated pipe; (——), resonator with the co-axial perforated pipes (see Figure 2).

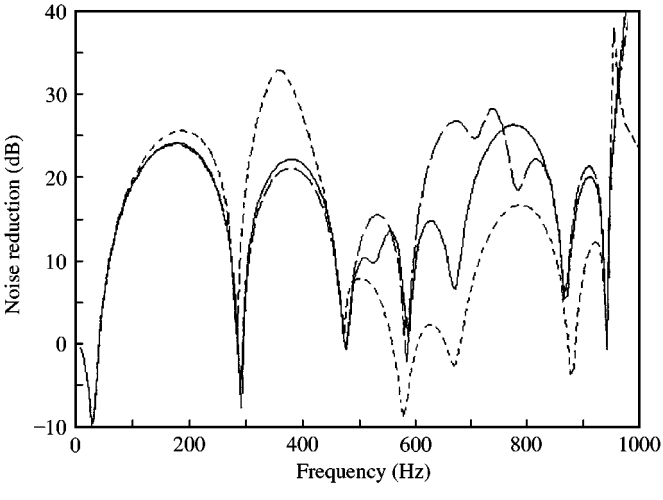

Figure 5. Effect of the diameter of the co-axial pipe on noise reductions. (– – –), $D_2 = 0{\cdot}1$ m; (— — —), $D_2 = 0{\cdot}153$ m; (——), $D_2 = 0{\cdot}175$ m,

changes that occur in the noise reduction characteristic of Figure 3 when the porosity of the co-axial pipe is taken as $\sigma_2 = 0{\cdot}01$ and its diameter is varied as $D_2 = 0{\cdot}1, 0{\cdot}153$ and $0{\cdot}175$ m. It is seen that increasing the diameter of the co-axial pipe improves the noise reduction for the higher frequencies, whilst decreasing it tends to improve it for the lower frequencies. In general, it is difficult to state general simple rules for the effects of the diameter and the size of the perforations of a low-porosity co-axial pipe; however, these can be predicted readily by using the present formulation.

Finally, shown in Figure 6 is the effect of mean flow on the noise reduction characteristic of Figure 3. These results assume zero mean flow in both annuli, that is, $M_1 = M_2 = 0$. As can be seen, the noise reduction of the resonator degrades with increasing mean flow in the

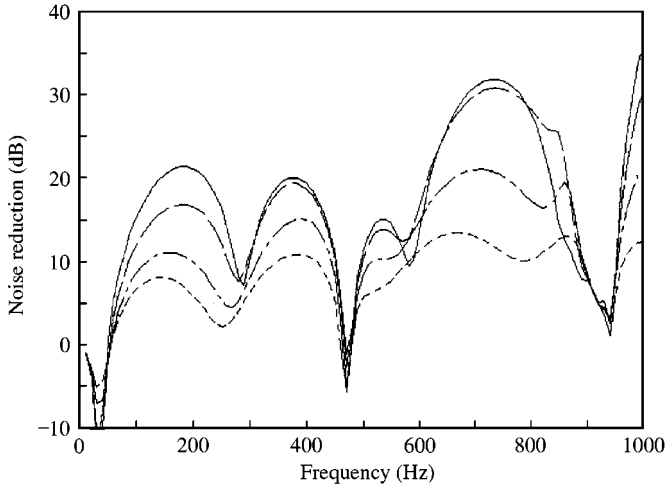

Figure 6. Effect of mean flow on the noise reduction of the co-axial resonator: $M_1 = M_2 = 0$, (——), $M_3 = 0{\cdot}05$; (— —), $M_3 = 0{\cdot}1$; (— - —), $M_3 = 0{\cdot}2$; (- - - -), $M_3 = 0{\cdot}3$.

central perforated pipe. This result could not be verified experimentally due to lack of facilities; however, it is confirmed by a different method in which the perforations are modelled discretely.

4. CONCLUSION

The distributed parameter method is extended for the analysis of mufflers employing concentric multiple pipes. Although the parallel pipe designs are more common in automotive applications, the co-axial designs may provide more compact solutions for some applications and can be easily provided with absorptive elements. The present formulation can be generalized for the presence of absorptive packings, and also for mufflers that employ a parallel pipe design where one or more of the pipes are multiple concentric perforated pipe elements.

Noise reduction is used in this analysis as an acoustic performance parameter mainly for the simplicity of its measurement. This depends, in addition to the resonator proper, on the inlet and outlet pipes. The loss of accuracy due to inclusion of the latter is negligible because, in the frequency range considered, the mathematical models used in the analysis can predict the sound transmission in such pipes accurately.

ACKNOWLEDGMENTS

The author wishes to express his thanks to Mr. E. Arslan for carrying out the tests described in this paper.

REFERENCES

1. P. O. A. L. Davies, M. Harrison and H. J. Collins 1997 *Journal of Sound and Vibration* **200**, 195–225. Acoustic modelling of multiple path silencers with experimental validations.

2. E. DOKUMACI 1996 *Journal of Sound and Vibration* **191**, 505–518. Matrizant approach to acoustic analysis of perforated multiple pipe mufflers carrying mean flow.
3. R. A. FRAZIER, W. J. DUNCAN and A. R. COLLAR 1963 *Elementary Matrices and Some Applications to Dynamics and Differential Equations*. Cambridge: Cambridge University Press.